A Time-Dependent Quantum Dynamical Study of the H + HBr Reaction†

Bina Fu and Dong H. Zhang*

State Key Laboratory of Molecular Reaction Dynamics and Center for Theoretical and Computational Chemistry, Dalian Institute of Chemical Physics, Chinese Academy of Sciences, Dalian, People's Republic of China 116023

Received: May 17, 2007

Time-dependent wave packet calculations were carried out to study the exchange and abstraction processes in the title reaction on the Kurosaki−Takayanagi potential energy surface (Kurosaki, Y.; Takayanagi, T. *J. Chem. Phys.* **2003**, *119*, 7838). Total reaction probabilities and integral cross sections were calculated for the reactant HBr initially in the ground state, first rotationally excited state, and first vibrationally excited state for both the exchange and abstraction reactions. At low collision energy, only the abstraction reaction occurs because of its low barrier height. Once the collision energy exceeds the barrier height of the exchange reaction, the exchange process quickly becomes the dominant process presumably due to its larger acceptance cone. It is found that initial vibrational excitation of HBr enhances both processes, while initial rotational excitation of HBr from $j_0 = 0$ to 1 has essentially no effect on both processes. For the abstraction reaction, the theoretical cross section at $E_c = 1.6$ eV is 1.06 Å^2, which is smaller than the experimental result of 3 ± 1 Å^2 by a factor of 2−3. On the other hand, the theoretical rate constant is larger than the experimental results by about a factor of 2 in the temperature region between 220 and 550 K. It is also found that the present quantum rate constant is larger than the TST result by a factor of 2 at 200 K. However, the agreement between the present quantum rate constant and the TST result improves as the temperature increases.

1. Introduction

Hydrogen abstraction and hydrogen exchange reactions of H with HX (X = halogen) have been of fundamental importance in the development and understanding of elementary chemical kinetics and reaction dynamics. A large number of studies of these reactions have been carried out since the landmark experiments of Bodenstein and co-workers[1] at the end of the 19th century. In the last two decades, extensive theoretical and experimental studies have been carried out on the FH_2 and ClH_2 systems,[2−8] which have played a pivotal role in our understanding of bimolecular chemical reaction in unprecedented detail at the ultimate microscopic level. The experimental study on the abstraction reaction

$$H + HBr \rightarrow H_2 + Br$$

and the exchange reaction

$$H' + HBr \rightarrow H'Br + H$$

have been largely focused on the determination of reaction rates and kinetic isotope effects. The reaction rates for the abstraction reaction and kinetic isotope effects for this reaction have been measured by several different groups.[9−15] Valentini and co-workers have also carried out experimental studies to measure integral cross sections for the reaction system at a collision energy of 1.6 eV and obtained a cross section of 3 ± 1 Å^2 for the abstraction reaction and a cross section of 11 ± 2 Å^2 for the combined energy transfer and reactive exchange processes.[16] Recently, Zare and co-workers measured the rotational state distribution for the reaction $H + HBr \rightarrow H_2 (v' = 2, j') + Br$ at a 53 kcal/mol collision energy and observed a small fraction of the H_2 molecule produced in highly rotationally excited states.[17] Based on quasi-classical trajectory (QCT) calculations on a London−Eyring−Polanyi−Sato (LEPS) potential energy surface, they discovered an indirect mechanism for the abstraction reaction in which the reaction proceeds through the bend transition states, in addition to the typical direct mechanism in which the reaction proceeds along the collinear reaction path.

Largely due to lack of an accurate potential energy surface for the system, there are only a very limited number of quantum dynamical studies carried out for the reactions so far. Clary et al. did some approximate quantum dynamical calculations for the H + HBr reaction on a LEPS functional potential energy surface (PES) in the 1980s.[18−20] A decade ago, Lynch et al. carried out multireference configuration interaction (MRCI) calculations with a large basis set for the ground-state PES for the BrH_2 system at 104 geometries preselected for convenient use in fitting an analytical PES via the extended LEPS function form with a three-center term.[21] Rate constants were calculated on the fitted analytical PES by using the improved canonical variational transition state theory and the least-action semiclassical tunneling approximation. It was found that the calculated rate constants for the abstraction reaction and its four deuterium and muonium isotopic variants were in good agreement with experimental results; however, the result would be further improved if the classical barrier height (1.9 kcal/mol) of the abstraction channel were lowered by 0.15−0.6 kcal/mol. However, the agreement with experiment is much less satisfactory for the exchange reactions, indicating that the barrier height of 12 kcal mol^{-1} should be lowered to improve the situation.

To further improve the PES presented by Lynch et al., Kurosaki and Takayanagi constructed a global adiabatic PES

† Part of the "Sheng Hsien Lin Festschrift".

* To whom correspondence should be addressed. E-mail: zhangdh@dicp.ac.cn.

10.1021/jp073811z CCC: $37.00
Published on Web 08/14/2007

of the lowest three doublet states ($1^2A'$, $2^2A'$, and $1^2A''$) using the MRCI method including the Davidson's correction with the aug-cc-pVTZ basis set and spin−orbit coupling effects.[22] The barrier height of the abstraction and exchange reactions on the ground-state PES are 1.28 and 11.71 kcal/mol, respectively, both of which are slightly smaller than the values obtained by Lynch et al.[21] Thermal rate constants calculated with the fitted $1^2A'$ PES agree better with experiment than those obtained by Lynch et al., although it was concluded that the barrier height was somewhat smaller than the true value. Therefore recently, Kurosaki and Takayanagi[23] presented a modified version of the $1^2A'$ PES with a barrier height for the abstraction reaction of 1.53 kcal/mol, compared to 1.28 kcal/mol on the original PES.[22] The transition state theory (TST) rate constants for the abstraction reaction and its isotopic variants on this newly constructed $1^2A'$ PES agree with experiment substantially better than the previous PES. So far, there are no quantum dynamical studies carried out on the newly modified PES; therefore, it is rather interesting to perform quantum dynamical studies to check the accuracy of TST for this reaction system and the accuracy of the PES, as well as to investigate the dynamical aspects of the reaction.

In this Article, we present a time-dependent (TD) wave packet study for the abstraction and exchange processes of the H + HBr reaction for the collision energy up to 2.0 eV on the Kurosaki−Takayanagi PES.[23] Accurate integral cross sections for the reaction are calculated, and the effect of rovibrational excitation of HBr on both processes is investigated. Comparisons are made between our theoretical results and available experimental measurements, when possible, to further verify the accuracy of the PES. To the best of our knowledge, this is the first quantum dynamics study on the PES. This Article is organized as follows. Section 2 gives a brief sketch of the TD method for atom−diatom reactive scattering used in the current study. The numerical details of our calculation and total reaction probabilities, cross sections, and rate constants for the reaction in the ground state, first excited rotational state, and vibrational state of HBr are reported in section 3. Comparisons of the rate constant of the abstraction reaction with experimental measurement are also discussed in this section. Section 4 gives a brief conclusion of the present work.

2. Theory

In this section, we briefly outline the TD wave packet approach to calculate the initial-selected total reaction probabilities. The reader is referred to refs 24 and 25 for more detailed discussions of the method. In reactant Jacobi coordinates, the Hamiltonian for the atom−diatom reaction H + HBr can be written as

$$H = -\frac{\hbar^2}{2\mu_R}\frac{\partial^2}{\partial R^2} + \frac{(\mathbf{J}-\mathbf{j})^2}{2\mu_R R^2} + \frac{\mathbf{j}^2}{2\mu_r r^2} + V(\mathbf{R},\mathbf{r}) + h(r) \quad (1)$$

where μ_R is the reduced mass between H and the center-of-mass of HBr, **J** is the total angular momentum operator, **j** is the rotational angular momentum operator of HBr, and $V(\mathbf{R},\mathbf{r})$ is the interaction potential excluding the diatomic potential of HBr. The diatomic reference Hamiltonian $h(r)$ is defined as

$$h(r) = -\frac{\hbar^2}{2\mu_r}\frac{\partial^2}{\partial r^2} + V(r) \quad (2)$$

where $V(r)$ is the diatomic potential for HBr.

The time-dependent wave function satisfying the Schrödinger equation is expanded in terms of the translational basis of R, vibrational basis $\phi_v(r)$, and the body-fixed (BF) total angular momentum eigenfunctions $\mathbf{Y}_{jK}^{JM\epsilon}$ as[24]

$$\Psi_{v_0 j_0 K_0}^{JM\epsilon}(\mathbf{R},\mathbf{r},t) = \sum_{n,v,j,K} F_{nvjK,v_0 j_0 K_0}^{JM\epsilon}(t) u_n^v(R)\phi_v(r) Y_{jK}^{JM\epsilon}(\hat{R},\hat{r}) \quad (3)$$

where u_n^v is translational basis function for R, which is dependent on v as given in ref 26, and (v_0, j_0, K_0) denote the initial rovibrational state of the system.

The BF total angular momentum basis $\mathbf{Y}_{jK}^{JM\epsilon}(\hat{R},\hat{r})$ quantities in eq 3 are the eigenfunctions for **J**, **j**, K, and the parity operator. They are defined as[24]

$$\mathbf{Y}_{jK}^{JM\epsilon} = (1+\delta_{K_0})^{-1/2}\sqrt{\frac{2J+1}{8\pi}}\left[D_{KM}^{J} + \epsilon(-1)^K D_{-KM}^{J}\right] y_{jK} \quad (4)$$

where $D_{K,M}^{J}$ is the Wigner rotation matrix, ϵ is the total parity of the system defined as $\epsilon = (-1)^{j+L+J}$, with L being the orbital angular momentum quantum number, $0 \le K \le \min(J, j)$ is the projection of total angular momentum on the BF axis, and y_{jK} is spherical harmonics. Note that in eq 4, the $K = 0$ block can only appear when $\epsilon = 1$.

As in refs 24 and 25, we construct initial wave packets and propagate them by using the split-operator method to calculate the reaction probabilities $P_{v_0 j_0 K_0}^{J\epsilon}(E)$ for each product. The integral cross section from a specific initial state (v_0, j_0) is obtained by summing the reaction probabilities over all of the partial waves (total angular momentum J)

$$\sigma_{v_0 j_0}(E) = \frac{1}{2j_0+1}\sum_{K_0\epsilon}\sigma_{v_0 j_0}^{K_0\epsilon}(E) = \frac{1}{2j_0+1}\sum_{K_0\epsilon}\left\{\frac{\pi}{k^2}\sum_{J\ge K_0}(2J+1)P_{v_0 j_0 K_0}^{J\epsilon}(E)\right\} \quad (5)$$

where $k = 2\mu E/\hbar$, and $\sigma_{v_0 j_0}^{K_0\epsilon}(E)$ is defined as the K_0- and ϵ-specified cross section. The initial state-specific reaction rate constant is calculated by thermally averaging the translational energy of the corresponding cross section as

$$k_{v_0 j_0}(T) = \left(\frac{8kT}{\pi\mu}\right)^{1/2}(k_b T)^{-2}\int_0^\infty \mathrm{d}E\, E\mathrm{e}^{-E/kT}\sigma_{v_0 j_0}(E) \quad (6)$$

where E is the translational energy, and k_b is the Boltzmann's constant. Finally, the thermal rate constant can be calculated from the Boltzmann averaging of the initial state-specific reaction rate constants as

$$k(T) = \frac{\sum_{v_0 j_0}(2j_0+1)\,k_{v_0 j_0}(T)\mathrm{e}^{-E_{v_0 j_0}/k_b T}}{\sum_{v_0 j_0}(2j_0+1)\mathrm{e}^{-E_{v_0 j_0}/k_b T}} \quad (7)$$

where $E_{v_0 j_0}$ is the rovibrational energy of the HBr molecule.

3. Results

The most recent potential of the ground state ($1^2A'$) constructed by Kurosaki and Takayanagi for the BrH_2 system is used in the present calculation.[23] The numerical parameters for the wave packet propagation are as follows. A total number of 250 sine functions (among them, 125 for the interaction region) are employed for the translational coordinate R in a range of

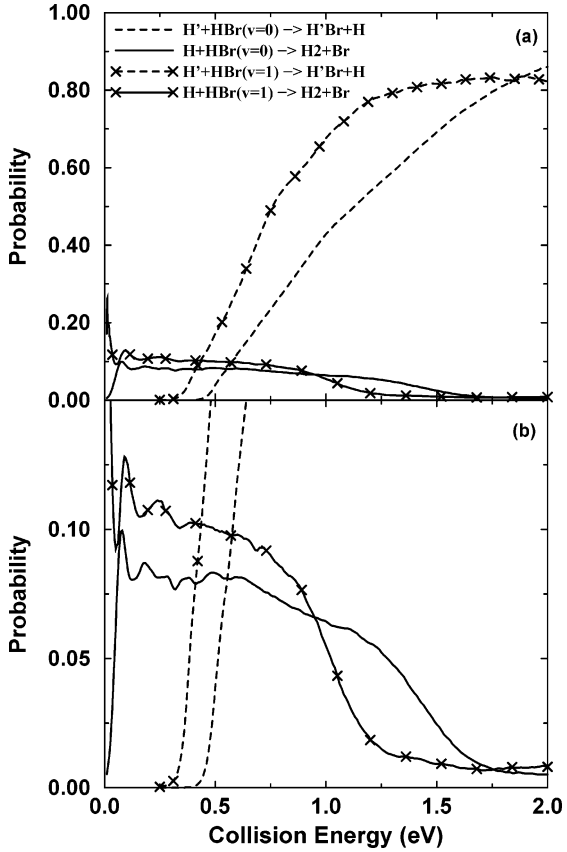

Figure 1. (a) Total reaction probabilities for $J = 0$ for the H + HBr ($v_0 = 0,1$, $j_0 = 0$) reaction as a function of collision energy; (b) same as (a) except showing the probability up to 15%.

[1.5,25]a_0. A total of 80 vibrational functions are employed for r in the range of [1.5,10]a_0 for the reagents HBr in the interaction region. For rotational basis, we use $j_{max} = 100$. We use up to 9 K blocks to compute accurate reaction probabilities for J up to 85 to get converged integral cross sections for the reaction. For lower J, we propagate the wave packets for 10000 au of time to converge the low-energy reaction probability. For $J > 20$, we propagate the wave packets for a shorter time because the reaction probability in the low-energy region is negligible.

The total reaction probabilities for the H + HBr ($v_0 = 0,1$) reaction as a function of the translational energy for the total angular $J = 0$ are presented in Figure 1a. First, we can see from the figure that the behavior of the reaction probabilities for the two channels is rather different. For the H + HBr ($v_0 = 0$) reaction, the threshold of the exchange reaction is about 0.42 eV, while the abstraction reaction has almost no threshold. This is due to the fact that the barrier height of the exchange reaction is 0.51 eV, and that of the abstraction reaction is much lower, only 0.066 eV for the PES[23] employed in this study. As the collision energy increases, the reaction probability for the exchange reaction increases steadily to a large value of more than 85%. From Figure 1b, we can see the reaction probability of the abstraction reaction rises from zero threshold, rapidly reaches the maximum value of 10% at a translational energy of about 0.08 eV, then remains about 8% up to $E_c = 0.6$ eV. In the energy region, the reaction probability exhibits some oscillatory structures, with a rather pronounced peak at $E_c = 0.078$ eV. As the collision energy increases from 0.6 to 1.2 eV, the abstraction reaction probability decreases gradually from 8 to about 5.5%. Then, it drops very quickly to about 0.6% at $E_c = 1.7$ eV and remains more or less flat as the collision energy increases further. Hence, at low collision energy, the abstraction reaction is the dominant process. Once the collision energy exceeds the barrier height of the exchange reaction, the exchange process becomes dominant quickly, presumably due to the fact that the exchange reaction has a larger acceptance cone than the abstraction reaction. It is also interesting to observe that the effect of translational energy on these two processes is very different. It enhances the exchange reactivity but hinders the abstraction reactivity.

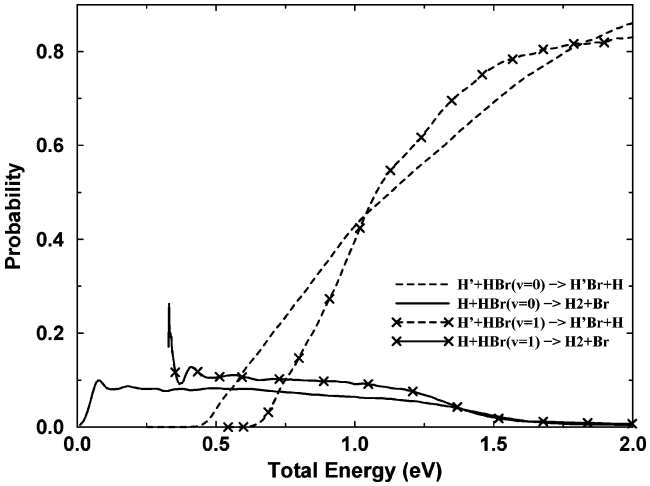

Figure 2. Same as Figure 1 except as a function of the total energy measured from the ground rovibrational state of HBr.

The vibrational excitation energy for HBr from $v_0 = 0$ to 1 is 0.318 eV on the PES used in this study. From Figure 1, we can see that the initial vibrational excitation of HBr enhances the exchange reactivity substantially, in particular in the medial energy region. The threshold energy for the process is reduced from 0.42 to 0.28 eV. Figure 2 shows the reaction probabilities as a function of the total energy measured from the ground rovibrational energy of HBr. It is interesting to see that for the total energy above 1.0 eV, the exchange probability for the HBr ($v_0 = 1$) initial state is actually larger than that for $v_0 = 0$ state, indicating that the vibrational excitation of HBr is more effective than the translational energy on prompting the exchange reaction in the energy region. For the abstraction reaction, there is no threshold for the HBr ($v_0 = 1$) initial state, as can be seen from Figure 1b. The overall behavior of the exchange probability for the $v_0 = 1$ state resembles that for the $v = 0$ state. The oscillatory structures in the very low collision region become more pronounced compared to that for the $v_0 = 0$ state. For a collision energy up to 1.0 eV, the probability for the $v_0 = 1$ state is larger than that for the $v_0 = 0$ state. However, as the collision energy increases further, the probability for the $v_0 = 1$ state decreases faster than that for the $v_0 = 0$ state and reaches the flat value of less than 1% at about 1.3 eV. Interestingly, if measured in the total energy as in Figure 2, both the $v_0 = 0$ and 1 abstraction probabilities start to decrease quickly from the same total energy of 1.2 eV and reach the flat value of less than 1% at about the same energy of 1.7 eV.

To obtain the integral cross sections for the reaction, we have calculated the reaction probabilities for a number of total angular momenta J. The energy dependence of the total reaction probabilities for the exchange and abstraction channels are shown in Figure 3a and b, respectively, for $J = 0$, 10, 20, 30, and 40. Figure 3 shows that with increasing J, the probabilities shift toward the higher energy because of the increasingly higher centrifugal barrier. However, the threshold of the exchange reaction moves much faster than that of the abstraction one due to the fact that the saddle point for the exchange channel has a

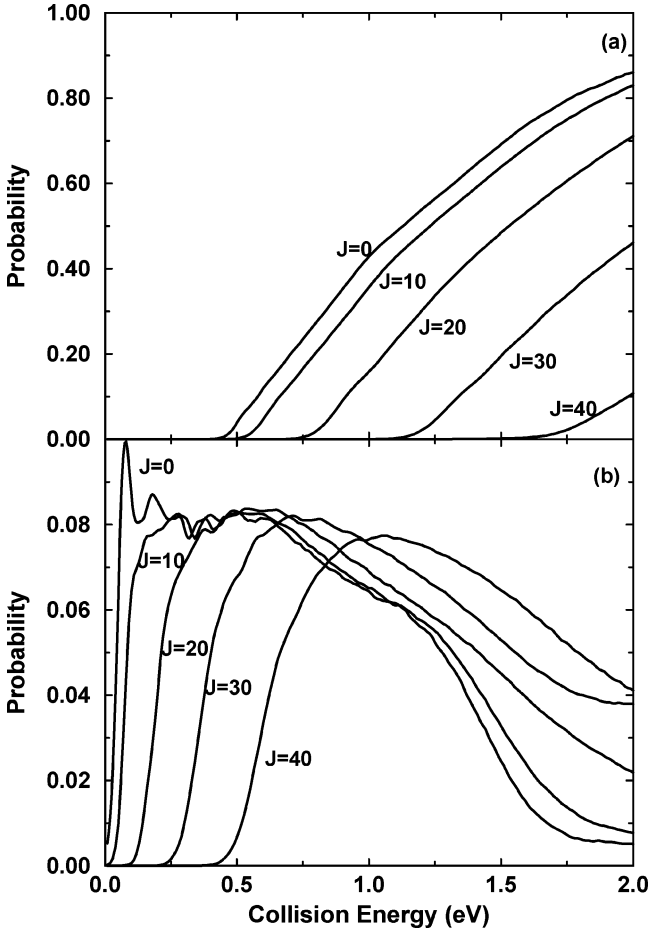

Figure 3. (a) Total reaction probabilities for $J = 0$, 10, 20, 30, and 40 for the H′ + HBr ($v_0 = 0$, $j_0 = 0$) → H + H′Br exchange reaction as a function of the collision energy; (b) same as (a) except for the H + HBr ($v_0 = 0$, $j_0 = 0$) → H_2 + Br abstraction reaction.

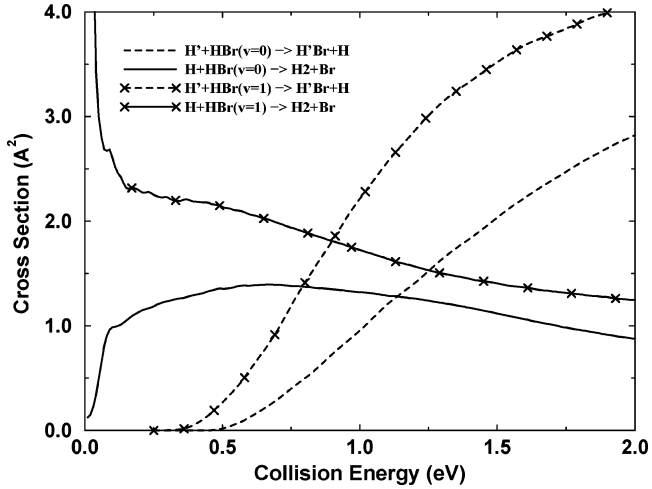

Figure 4. Integral cross sections for the H + HBr ($v_0 = 0,1$, $j_0 = 0$) reaction as a function of collision energy.

small value of R compared to that of the abstraction reaction. It can be seen from Figure 3 that for a fixed collision energy, the exchange reaction probabilities decrease monotonically with an increase of J in the entire energy region, while the abstraction reaction probabilities at high collision energy actually increase with the increase of J for small values of J.

The integral cross sections for the H + HBr ($v_0 = 0,1$) reactions are depicted in Figure 4. The exchange cross sections for both initial states increase monotonically with an increase

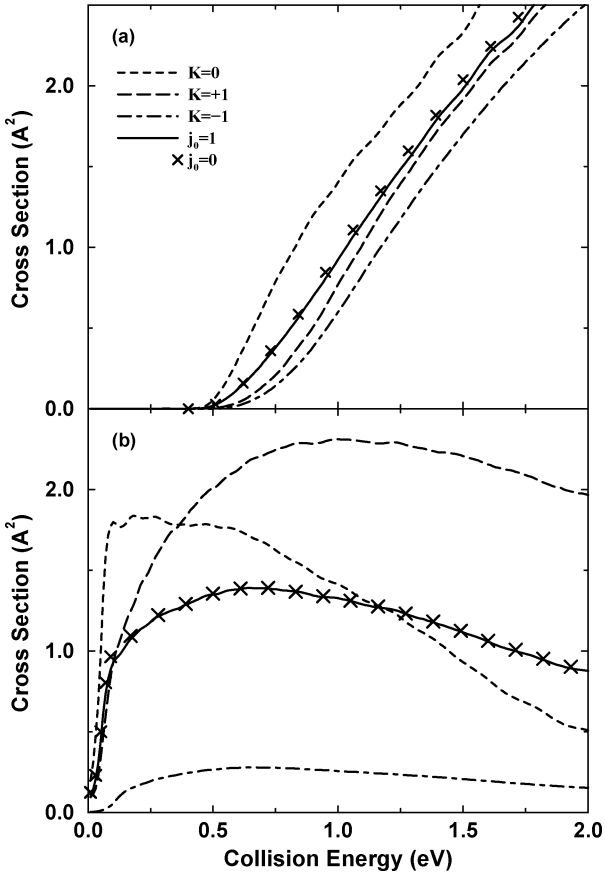

Figure 5. (a) K_0- and ϵ-specified and total cross sections for the H′ + HBr ($v_0 = 0$, $j_0 = 0,1$) → H + H′Br exchange reaction; (b) same as (a) except for the H + HBr ($v_0 = 0$, $j_0 = 0$) → H_2 + Br abstraction reaction.

of translational energy. In contrast, the abstraction cross section for the $v_0 = 1$ initial state decreases monotonically with the increase of collision energy. For the $v_0 = 0$ initial state, the abstraction cross section increases very rapidly to a value of 1.0 Å^2 at $E_c = 0.1$ eV, then slowly increases to the maximum value of 1.4 Å^2 at $E_c = 0.7$ eV, and finally decreases slowly with the further increase of collision energy to a value of 0.88 Å^2 at $E_c = 2.0$ eV. At $E = 1.6$ eV, the integral cross section for the reaction is 1.06 Å^2, which is smaller than the experimental result of 3 ± 1 Å^2 by a factor of 2−3. [16,27]

It can be seen clearly from Figure 4 that the abstraction reaction is the dominant process for the collision energy up to 1.0 eV, which is substantially higher than the cross point of 0.55 eV for the abstraction and exchange reaction probabilities for $J = 0$ shown in Figure 1b. At high collision energy, the abstraction probability is almost negligible compared to the exchange probability, as shown in Figure 1a, while for the cross section, the abstraction reaction is only smaller than the exchange reaction by a factor of 3 at $E_c = 2.0$ eV. Finally, we can see from Figure 4 that the initial vibration excitation of HBr enhances both the exchange and abstraction cross sections in the entire energy region considered in this study, although in the high collision region, the enhancement of the abstraction cross section is not substantial.

Figure 5 shows the K_0- and parity (ϵ)-specified cross sections for the H + HBr ($j_0 = 1$) reaction, with $K = 0$ denoting the $K_0 = 0$, $\epsilon = +1$ initial state and $K = \pm 1$ denoting the $K_0 = 1$, $\epsilon = \pm 1$ initial states, respectively. For the exchange reaction shown in Figure 5a, in the entire energy region, the $K = 0$ cross section is the largest one, and the $K = \pm 1$ cross section is slightly larger than the $K = -1$ one. Although in the low-

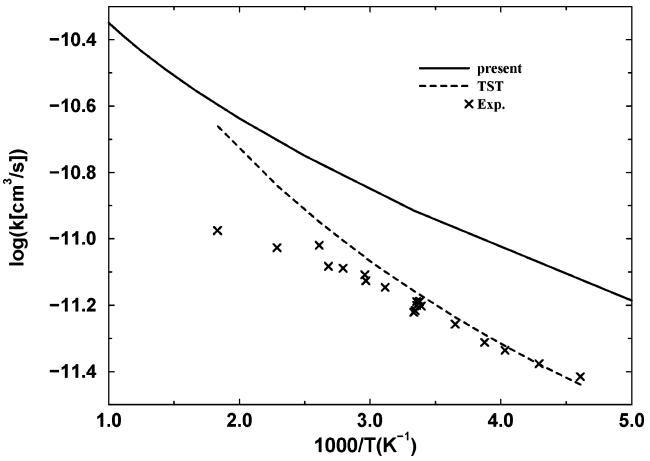

Figure 6. Initial state-selected rate constant for the H + HBr ($v_0 = 0$, $j_0 = 0$) → H_2 + Br abstraction reaction, in comparison with the TST thermal rate constant[23] and experimental measurements.[9−13]

collision-energy region the $K = 0$ cross section is substantially larger than the other two, the cross sections for these three initial states are quite close to each other overall. In contrast, the abstraction cross sections strongly depend on the initial K_0 and ϵ, as shown in Figure 5b. The $K = 0$ cross section increases rapidly to the maximum value of 1.8 Å^2 at $E_c = 0.1$ eV, then decreases quickly when $E_c > 0.5$ eV, and drops down to 0.5 Å^2 at $E_c = 2.0$ eV. The $K = +1$ cross section increases steadily to the maximum value of 2.3 Å^2 at $E_c = 1.0$ eV and then decreases slightly as the collision energy increases further, reaching 2.0 Å^2 at $E_c = 2.0$ eV. On the other hand, the maximum value for the $K = -1$ cross section is merely 0.28 Å^2 at $E_c = 0.7$ eV, substantially smaller than the corresponding values of the other two states.

By averaging the $K = 0$ and ± 1 cross sections, we can obtain the integral cross section for the H + HBr ($j_0 = 1$) reaction shown in Figure 5, in comparison with that for the H + HBr ($j_0 = 0$) reaction. Interestingly, both the exchange and abstraction cross sections for the H + HBr ($j_0 = 1$) reaction are almost identical to the corresponding cross sections for the $j_0 = 0$ reaction, despite the fact that the K_0- and parity (ϵ)-specified cross sections, in particular those for the abstraction reaction, vary dramatically for different initial states.

Figure 6 shows the initial state-selected rate constant of the H + HBr ($v_0 = 0$, $j_0 = 0$) → H_2 + Br reaction in the range of temperatures between 200 and 1000 K, in comparison with thermal rate constants for the abstraction reaction obtained from a transition state theory (TST) study[23] and experiments.[9−13] Because the vibrational excitation energy of HBr is quite high (0.318 eV), the population for the vibrationally excited state is negligible in the temperature region considered. In addition, based on the fact that the abstraction cross section for the $j_0 = 1$ state is very close to that for the $j_0 = 0$, we assume rotational excitation of HBr has little effect to the rate constant of the reaction. Hence, we expect that the rate constant for the initial ground rovibrational reactant state should be close to the thermal rate constant in the temperature region considered here. As can seen from Figure 6, the thermal rate constant for the abstraction reaction is not sensitive to temperature. As the temperature increases from 200 to 1000 K, it only increases by a factor of 7 because of the weak dependence of the abstraction cross section on the collision energy, as shown in Figure 4. It can be seen that the slope of the present abstraction rate constants agrees with the experimental result very well, with the present theoretical result larger than the experimental measurements roughly by a factor of 2 for the temperature up to 550 K. Interesting, the TST rate constant agrees with the experimental result very well in the low-temperature region. However, as the temperature increases, the deviation between the TST result and experiment increases, and the TST result approaches the present quantum mechanical (QM) rate constant. At $T = 550$ K, the QM rate constant is only 16% large than the TST result. The discrepancy between the present QM result and the TST result is likely caused by neglecting the quantum tunneling effect in the TST result, which can have a substantial effect to the rate constant in the low-temperature region. From the comparison between the present QM result and the experiment, we can see that one needs to improve the PES that we employed in this calculation in order to achieve better agreement between theory and experiment.

4. Conclusion

We have carried out a quantum dynamic study on the H + HBr reaction using the TD wave packet approach on the potential energy surface of Y. Kurosaki and T. Takayanagi.[23] We calculated the total reaction probabilities and cross sections of both channels for the H + HBr reaction for the collision energy up to 2.0 eV and studied the influence of the initial rotational and vibrational state excitation of the reagents on the reaction. The lower reaction barrier for the abstraction reaction makes it easier to occur in the low-collision-energy region. Once the collision energy exceeds the exchange reaction barrier, the exchange process quickly becomes dominant, presumably due to the fact that the exchange reaction has a larger acceptance cone than that of the abstraction reaction. It is found that the initial vibrational excitation of HBr enhances both processes, while initial rotational excitation of HBr from $j_0 = 0$ to 1 has essentially no effect on both processes. For the $j_0 = 1$ initial state, strong dependence of the cross section on initial K_0 and parity is observed for the abstraction process but not for the exchange process.

For the abstraction reaction, the theoretical cross section at $E_c = 1.6$ eV on this PES is 1.06 Å^2, which is smaller than the experimental result of 3 ± 1 Å^2 by a factor of 2−3.[16,27] On the other hand, the theoretical rate constant is larger than the experimental results by a factor of 2 for temperatures up to 550 K. Hence, it is conceivable that the Kurosaki−Takayanagi PES underestimates the barrier height and acceptance cone for the abstraction reaction. The PES should be further improved in order to achieve better agreement between theory and experiment.

Acknowledgment. This work is supported by the Knowledge Innovation Program of the Chinese Academy of Science (Grants DICP R200402 and Y200601) and by NSFC (Grant No. 20688301). We thank Dr. Kurosaki for sending us the PES used in this study.

References and Notes

(1) Bodenstein, M. *Z. Phys. Chem.* **1899**, *29*, 295.
(2) Neumark, D. M.; Wodtke, A. M.; Robinson, G. N.; Haygen, C. C.; Lee, Y. T. *Phys. Rev. Lett.* **1984**, *54*, 229.
(3) Stark, K.; Werner, H.-J. *J. Chem. Phys.* **1996**, *104*, 6515.
(4) Castillo, J. F.; Manolopoulos, D. E.; Stark, K.; Werner, H.-J. *J. Chem. Phys.* **1996**, *104*, 6531.
(5) Castillo, J. F.; Hartke, B.; Werner, H.-J.; Aoiz, F. J.; Bañares, L.; Matínez-Haya, B. *J. Chem. Phys.* **1998**, *109*, 7224.
(6) Qiu, M.; Ren, Z.; Che, L.; Dai, D.; Harich, S. A.; Wang, X.; Yang, X.; Xu, C.; Dai, D.; Gusatafsson, M.; Skodje, R. T.; Sun, Z.; Zhang, D. H. *Science* **2006**, *311*, 1440.
(7) Bian, W.; Werner, H.-J. *J. Chem. Phys.* **2000**, *112*, 220.

(8) Skouteris, D.; Manolopoulos, D. E.; Bian, W.; Werner, H.-J.; Lai, L.-H.; Liu, K. *Science* **1999**, *286*, 1713.
(9) Talukdar, R. K.; Warren, F. R.; Vaghijiani, G. L.; Ravishankara, A. R. *Int. J. Chem. Kinet.* **1992**, *24*, 973.
(10) Seakins, P. W.; Pilling, M. J. *J. Phys. Chem.* **1991**, *95*, 9878.
(11) Jourdain, J. L.; Bras, G. L.; Combourieu, J. *Chem. Phys. Lett.* **1981**, *78*, 483.
(12) Mitchell, T. J.; Gonzalez, A. C.; Benson, S. W. *J. Phys. Chem.* **1995**, *99*, 16960.
(13) Hussian, D.; Slater, N. K. H. *J. Chem. Soc., Faraday Trans. 2* **1980**, *76*, 276.
(14) Umemoto, H.; Wada, Y.; Tsunashima, S.; Takayanagi, T.; Sato, S. *Chem. Phys.* **1990**, *143*, 333.
(15) Gonzalez, A. C.; Tempelmann, A.; Arseneau, D. J.; Fleming, D. G.; Senba, M.; Kempton, J. R.; Pan, J. J. *J. Chem. Phys.* **1992**, *97*, 6309.
(16) Aker, P. M.; Germann, G. J.; Valentini, J. *J. Chem. Phys.* **1989**, *90*, 4795.
(17) Pomerantz, A. E.; Camden, J. P.; Chiou, A. S.; Ausfelder, F.; Chawla, N.; Hase, W. L.; Zare, R. N. *J. Am. Chem. Soc.* **2005**, *127*, 16368.
(18) Clary, D. C. *J. Chem. Phys.* **1982**, *71*, 117.
(19) Clary, D. C.; Garrett, B. C.; Truhlar, D. G. *J. Chem. Phys.* **1983**, *78*, 777.
(20) Clary, D. C. *J. Chem. Phys.* **1985**, *83*, 1685.
(21) Lynch, G. C.; Truhlar, D. G.; Brown, F. B.; Zhao, J.-G. *J. Phys. Chem.* **1995**, *99*, 207.
(22) Kurosaki, Y.; Takayanagi, T. *J. Chem. Phys.* **2003**, *119*, 7838.
(23) Kurosaki, Y.; Takayanagi, T. *Chem. Phys. Lett.* **2005**, *406*, 121.
(24) Zhang, D. H.; Zhang, J. Z. H. *J. Chem. Phys.* **1994**, *101*, 3671.
(25) Zhang, D. H.; Lee, S. Y.; Bear, M. *J. Chem. Phys.* **2000**, *112*, 9802.
(26) Zhang, D. H.; Zhang, J. Z. H. *J. Chem. Phys.* **1994**, *101*, 1146.
(27) Aker, P. M.; Germann, G. J.; Tabor, K. D.; Valentini, J. *J. Chem. Phys.* **1989**, *90*, 4809.